



ChemComm

Pillar[6]quinone: Facile Synthesis, Crystal Structures and Electrochemical Properties

Journal:	<i>ChemComm</i>
Manuscript ID	CC-COM-05-2021-002413.R1
Article Type:	Communication

SCHOLARONE™
Manuscripts

COMMUNICATION

Pillar[6]quinone: Facile Synthesis, Crystal Structures and Electrochemical Properties

Received 00th January 20xx,
Accepted 00th January 20xx

Tomoki Hirohata,^a Naoki Shida,^a Hidehiro Uekusa,^b Nobuhiro Yasuda,^c Hirotomoto Nishihara,^d
Tomoki Ogoshi,^e Ikuyoshi Tomita,^a and Shinsuke Inagi^{*a,f}

DOI: 10.1039/x0xx00000x

A novel electron-deficient macrocycle, pillar[6]quinone (P[Q]₆), has been synthesized for the first time by both chemical and electrochemical oxidation of pillar[6]arene, showing clear hexagonal columnar stacking in the solid state. Cathodic voltammetric studies of P[Q]₆ revealed that three electrons are injected first, followed by stepwise one-electron reductions.

Pillar[n]arenes (n: number of units), macrocyclic para-arylene methylene molecules, have attracted attention owing to their symmetrical macrocyclic structures with flexible molecular designs including side chains.¹ Among a number of macrocyclic molecules, pillar[n]arenes are considered to be unprecedented host molecules for small molecular guests.² Similarly, their quinone counterparts, pillar[n]quinones, are also fascinating molecules, which have a different electronic state, i.e., an electron-deficient nature derived from the quinone structure. Indeed, pillar[5]quinone (P[Q]₅) has shown interesting electrochemical behavior for reduction, namely multistep electron-capture in a macrocycle even in its non-conjugated structure.³ It is a potential candidate for organic cathode materials in alkali metal ion batteries.⁴ A more symmetrical molecule, pillar[6]quinone (P[Q]₆), is expected to form densely packed structures, but has not been synthesized to date. Recently 1,4-dihoxypillar[6]arenes with one to four arenes replaced by quinones have been reported,⁵ but the synthesis of P[Q]₆ still remains a challenge.

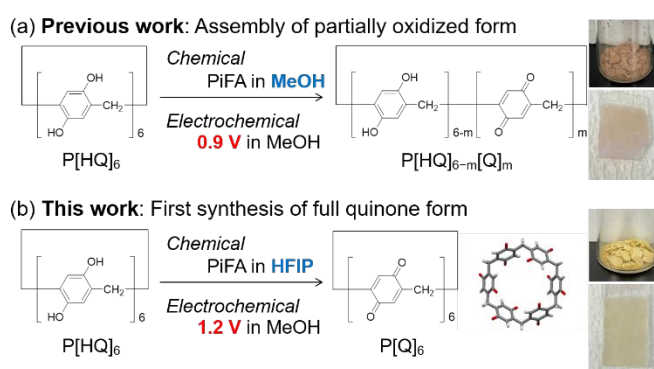


Fig. 1 Concept of this study. (a) Chemical or electrochemical oxidation of P[HQ]₆ in MeOH afforded the partially oxidized form P[HQ]_{6-m}[Q]_m in previous studies. (b) In the current study, chemical oxidation in HFIP or electrochemical oxidation at a higher potential gives the fully oxidized form P[Q]₆ for the first time.

In this study, we discovered that the synthesis of P[Q]₆ could be achieved by a simple electrochemical oxidation of 1,4-dihoxypillar[6]arene (P[HQ]₆) as shape-controlled deposits on an electrode surface (see the ESI,† Fig. S2). The chemical and crystalline structures were successfully characterized spectroscopically. We previously conducted electrochemical oxidation of P[HQ]₆ in methanol to give a hexagonal cylindrical deposition of partially oxidized P[HQ]_{6-m}[Q]_m (composed of both hydroquinone and quinone units) driven by aggregation via quinhydrone formation (Fig. 1a).⁶ In the current study, the application of a higher anodic potential for P[HQ]₆ was successful to achieve the oxidation of P[HQ]₆ to P[Q]₆. Inspired by this electrochemical method, we also developed a scalable method for preparing P[Q]₆ by chemical oxidation (Fig. 1b). This new macrocycle with high symmetry would be a potential candidate for new kinds of redox materials for energy device applications.

In our previous report,⁶ potentiostatic anodic oxidation (1.0 V vs. SCE) of P[HQ]₆ in a methanol solution containing tetrabutylammonium hexafluorophosphate (Bu₄NPF₆) gave hexagonal cylindrical structures of the charge-transfer (CT) complex of partially oxidized molecules (P[HQ]_{6-m}[Q]_m) on an ITO working electrode. The partially oxidized structure was characterized by IR

^a Department of Chemical Science and Engineering, School of Materials and Chemical Technology, Tokyo Institute of Technology, 4259 Nagatsuta-cho, Midori-ku, Yokohama 226-8502, Japan. E-mail: inagi@cap.mac.titech.ac.jp

^b Department of Chemistry, School of Science, Tokyo Institute of Technology, 2-12-1, Ookayama, Meguro-ku, Tokyo 152-8551, Japan

^c Diffraction and Scattering Division, Japan Synchrotron Radiation Research Institute, 1-1-1, Kouto, Sayo-gun, Hyogo 679-5198, Japan

^d Advanced Institute for Materials Research, Institute of Multidisciplinary Research for Advanced Materials, Tohoku University, 2-1-1, Katahira, Aoba-ku, Sendai 980-8577, Japan

^e Department of Synthetic and Biological Chemistry, Graduate School of Engineering, Kyoto University, Katsura, Nishikyo-ku, Kyoto 615-8510, Japan

^f PRESTO, Japan Science and Technology Agency (JST), 4-1-8 Honcho, Kawaguchi, Saitama 332-0012, Japan.

†Electronic Supplementary Information (ESI) available. See

DOI: 10.1039/x0xx00000x

and UV-vis analyses. Varying the applied potential (1.2 V and 1.4 V vs.

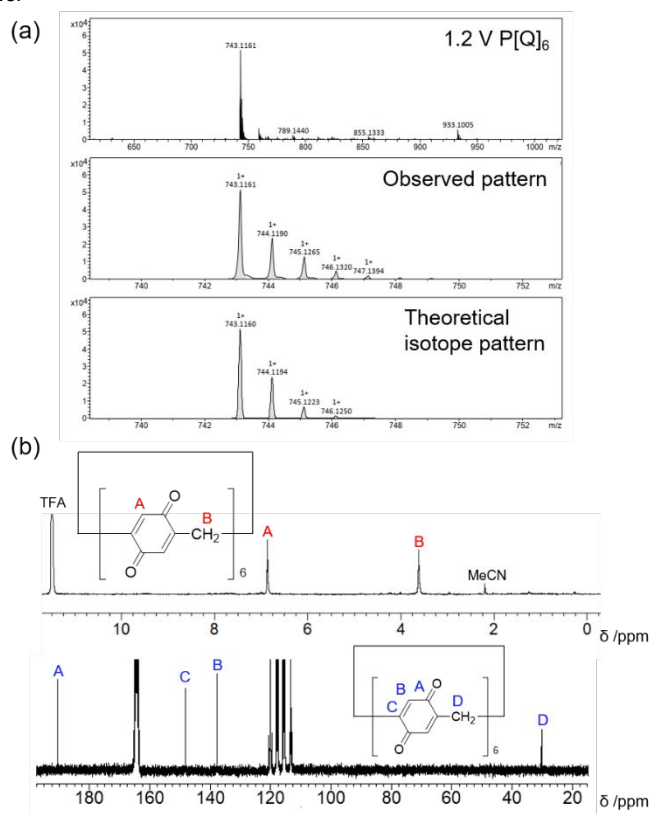


Fig. 2 (a) ESI-TOF-MS spectra of P[Q]₆ in HFIP. (b) ¹H NMR (upper) and ¹³C NMR (lower) spectra of P[Q]₆ measured in TFA-*d*.

SCE) was effective for controlling the size and length of the cylindrical structure. In the present study, we focused on deposits obtained by applying 1.2 V vs. SCE because they were colorless, indicating no CT interaction. The deposits obtained by electrochemical oxidation in methanol were not soluble in common organic solvents, making it difficult to characterize their chemical structures. However, by carefully investigating suitable solvents for the deposits, it was found that they were soluble in 1,1,1,3,3,3-hexafluoro-2-propanol (HFIP) and trifluoroacetic acid (TFA). These fluorinated alcohol and acid are known to have high proton donating abilities to dissolve quinone derivatives such as P[Q]₅.⁷ Therefore, spectroscopic analyses are possible for characterization of the deposits. First, electrospray ionization time-of-flight mass spectrometry (ESI-TOF-MS) was performed for the sample dissolved in HFIP. A molecular ion peak was observed at 743.1161 [M+Na⁺], which is assignable to P[Q]₆. The observed and theoretical isotope patterns were identical (Fig. 2a). On the other hand, ESI-TOF-MS of the samples prepared by electrochemical oxidation at 0.9 V vs. SCE or chemical oxidation in methanol⁸ showed complex isotope patterns, suggesting that the samples were composed of a complex mixture of partially oxidized P[HQ]_{6-m}[Q]_m (Fig. S3, ESI[†]).

NMR measurements were also carried out for the samples in TFA-*d*. The ¹H NMR spectrum of P[Q]₆ exhibited two sharp signals assignable to CH at 6.86 ppm and methylene CH₂ at 3.61 ppm. In the ¹³C NMR spectrum of P[Q]₆, characteristic signals at 190.5 (C=O), 148.1 (C-CH₂), 137.8 (CH) and 30.1 (CH₂) ppm clearly appeared (Fig. 2b). These results strongly support the highly symmetrical structure

of P[Q]₆ obtained by the above method. Since there was no signal for the ammonium salt in the NMR spectrum, it was determined that the

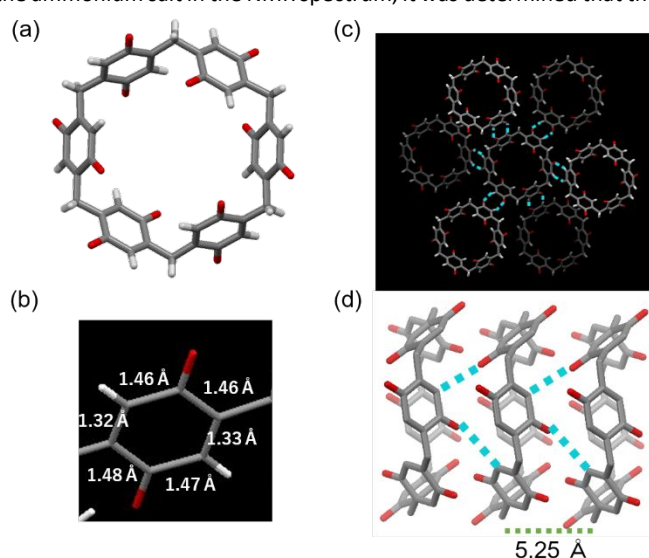


Fig. 3 Single-crystal X-ray structures of P[Q]₆: (a) top view, (b) bond lengths for a benzoquinone unit, (c) 2D packing structure with CH–O interactions (blue dotted lines) between adjacent quinones in the different layers, and (d) stacking columnar structure stabilized by intermolecular CH–O interactions (blue dotted lines).

deposited crystal did not incorporate the supporting electrolyte used for electrochemical oxidation.

A P[Q]₆ hexagonal cylindrical crystal (ca. 4 × 4 × 22 μm) prepared on an electrode surface was successfully mounted for single crystal X-ray diffraction (SCXRD) analysis. As seen in the crystal structure in Fig. 3b, the macrocycle is composed of six quinone units with bond lengths of 1.46–1.48 and 1.32–1.33 Å. The orientation of the quinone units in the macrocycle was not perpendicular but was aligned at around 35 degrees from the main axis (Fig. 3a), which is different from the case for other pillar[n]arene molecules.⁹ All quinone moieties seem to have intermolecular CH–O interactions between adjacent macrocycles, resulting in the formation of a hexagonal packing structure (Fig. 3c).

A columnar stacking structure is observed with an interval length of 5.25 Å, which is considerably shorter than that for the P[HQ]₆ crystal structure (9.21 Å).⁹ Multiple inter-columnar CH–O interactions presumably stabilize the tilted conformation of the macrocycles and contributes to their short-distance stacking (Fig. 3d). In the center of the columnar stacking structure, a continuous void was formed, which made this crystal a porous honeycomb structure. The diameter of this channel is ca. 7.89 Å, allowing it to incorporate small molecules such as methanol or gas molecules. However, no molecules were observed in the channel. Thus, neither Bu₄NPF₆ nor methanol was included in this structure. The hexagonal packing and columnar stacking of P[Q]₆ derived from multiple CH–O interactions probably contribute to the formation of the uniform hexagonal cylinder structure on the micrometer scale. It is noted that these interactions account for the poor solubility of the deposits in common organic solvents and good solubility in fluorinated alcohol and acid.

Theoretical calculations of P[Q]₆ were performed using density functional theory (DFT) by Yu and coworker.¹⁰ The calculated data for P[Q]₆ showed a highly symmetrical pillar-like structure. Our

calculations using DFT at the ω B97XD/6-311G+ (d,p) level of theory for P[Q]₆ starting with its crystal structure well converged to a local minimum energy (Fig. S6, ESI[†]). The difference in energy between the distorted structure and the pillar-like symmetrical structure was very small. In contrast, the pillar-like structure was much more stable for P[HQ]₆, presumably due to intramolecular hydrogen bond formation in P[HQ]₆ (Fig. S7, ESI[†]). Thus, the conformation of the P[Q]₆ macrocycle should be more flexible than that of P[HQ]₆, since it can adjust its conformation by multiple CH–O interactions in the solid state.

To produce a large amount of P[Q]₆, chemical synthesis is preferred over electrochemical deposition on an electrode surface. When P[HQ]₆ was treated with phenyliodine (III) bis(trifluoroacetate) (PIFA) as an oxidant in methanol, partially oxidized P[HQ]_{6-m}[Q]_m was deposited from a methanol solution before completing oxidation of P[HQ]₆.⁸ Kaifer and coworkers reported that oxidation of 1,4-diethoxypillar[6]arene with cerium (IV) ammonium nitrate (CAN) was successful to give quinone units in the macrocycle. However, they could isolate only a series of partially oxidized materials containing one to four quinone units.⁵ Here, with good solvents for P[Q]₆ in hand, we investigated the chemical oxidation of P[HQ]₆ with PIFA in HFIP (Fig. 1b). It was expected that the oxidation power of PIFA should be enhanced in HFIP as reported for a similar hypervalent iodoarene reagent.¹¹ P[HQ]₆ was dispersed in HFIP and an excess amount of PIFA was added. The reaction mixture turned into a clear orange-colored solution after several hours. Simple purification afforded pure P[Q]₆ as a yellow solid in good yield (80%) on a ca. 0.4 g scale. ¹H and ¹³C NMR, and ESI-TOF-MS spectra of chemically prepared P[Q]₆ were fully identical to those of electrochemically prepared P[Q]₆. In the UV-vis absorption spectrum of P[Q]₆ in HFIP, an absorption maximum was observed at 250 nm without significant CT bands at longer wavelengths (Fig. S9, ESI[†]). Although a single crystal of the chemically synthesized P[Q]₆ has not been obtained at the present time, its powder XRD (PXRD) pattern showed characteristic peaks, which are identical to that of the electrochemically prepared P[Q]₆ sample (Fig. S10 and S12, ESI[†]).

P[Q]₆ is expected to form a new class of redox active macrocycles. Various voltammetry techniques were performed for P[Q]₆ in dimethylformamide (DMF). First, the cyclic voltammogram (CV) of P[Q]₆ measured in 0.1 M Bu₄NPF₆/DMF showed several reversible redox couples in a negative scan from 0 to –2.0 V vs. Ag/Ag⁺ (Fig. 4a). To better understand the electron-transfer (ET) behavior, square wave voltammetry was carried out under the same conditions. In the square wave voltammogram (SWV) (Fig. 4b), the reduction responses were clearly distinguished in a similar potential area with a large redox couple at –0.8 V and small couples at –1.1 V, –1.3 V, –1.6 V. Normal pulse voltammetry can provide information on the number of electrons involved in the ET process. From the normal pulse voltammogram (NPV) (Fig. 4c), it was indicated that the same number of electrons was used in the two potential regions, i.e., –0.50 V– –1.05 V and –1.05 V– –1.70 V, in the reduction process of P[Q]₆. From these results, a possible ET mechanism for P[Q]₆ in aprotic media is proposed as follows (Fig. 4d). One-electron reduction of three quinone units in P[Q]₆ alternately occurs before –1.05 V, then the remaining three quinone units are reduced one by one at –1.05 through –1.7 V with divided peaks (in CV and SWV) due to the electrostatic repulsion in the second ET process. When the potential

scan was conducted in a more negative range up to –2.5 V, no reduction peak was observed in SWV and NPV. Considering the

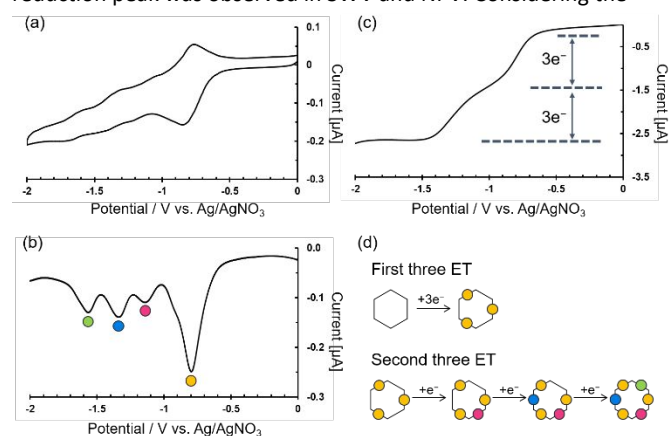


Fig. 4 (a) Cyclic voltammogram, (b) square wave voltammogram and (c) normal pulse voltammogram of 1 mM P[Q]₆ in 0.1 M Bu₄NPF₆/DMF, measured with a GC disk working electrode (ϕ = 1 mm), a Pt counter electrode (10 mm \times 10 mm) and an Ag/Ag⁺ reference electrode at a scan rate of 20 mV s⁻¹. (d) A schematic model for reduction of P[Q]₆ based on the voltammetric studies. The colored circles represent electrons injected into P[Q]₆, which are also coded on reduction waves in (b).

voltammetry analyses for para-xyloquinone (XQ) as a model compound (Fig. S14 and S15, ESI[†]), dianion formation of the quinone units in P[Q]₆ should occur at a more negative potential due to the electrostatic repulsion upon the injection of an electron into already charged P[Q]₆. Such multistep reduction behavior was also observed in P[Q]₅,³ but the symmetrical hexagonal structure of P[Q]₆ could accept three electrons at the same potential in an alternate manner.

In conclusion, we have successfully synthesized and characterized P[Q]₆ for the first time, by employing both chemical oxidation of P[HQ]₆ in HFIP and electrochemical oxidation of P[HQ]₆ at higher potential. In the latter case, hexagonal cylindrical crystals were easily obtained on an electrode surface. These could be readily transferred for single-crystal X-ray analysis, which clearly showed a hexagonal columnar structure. The CV, SWV and NPV studies on P[Q]₆ in DMF revealed that three electrons are injected first, followed by three one-electron reductions that occur stepwise. Since P[Q]₆ is a novel class of host molecule and redox active material, this study is expected to contribute to the exploration of a wide variety of related chemistry.

This research was supported by a Kakenhi Grant-in-Aid Grant (JP18H04504, JP20H04661 and JP20H02796) from the Japan Society for the Promotion of Science (JSPS), and a Support for Tokyo Tech Advanced Researchers [STAR] grant funded by the Tokyo Institute of Technology Fund (Tokyo Tech Fund). The synchrotron radiation experiment was performed at the BL40XU of SPring-8 with the approval of the Japan Synchrotron Radiation Research Institute (JASRI) (Proposal No. 2019A2016). We acknowledge Prof. Ryoji Kanno, Dr. Kota Suzuki and Dr. Naoki Matsui for XRD measurements. T.H. acknowledges a support from the Kato Foundation for Promotion of Science (KS-3304). The theoretical calculations were carried out on the TSUBAME3.0 supercomputer at Tokyo Institute of Technology supported by the MEXT Project of the Tokyo Tech Academy for Convergence of Materials and Informatics (TAC-MI).

Notes and references

- 1 a) T. Ogoshi, S. Kanai, S. Fujinami and T. Yamagishi, *J. Am. Chem. Soc.*, 2008, **130**, 5022–5023; b) P. J. Cragg and K. Sharma, *Chem. Soc. Rev.*, 2012, **41**, 597–607; c) N. L. Strutt, H. Zhang, S. T. Schneebeli and J. F. Stoddart, *Acc. Chem. Res.*, 2014, **47**, 2631–2642; d) T. Kakuta, T. Yamagishi and T. Ogoshi, *Chem. Commun.*, 2017, **53**, 5250–5266; e) T. Ogoshi, T. Kakuta and T. Yamagishi, *Angew. Chem. Int. Ed.*, 2019, **58**, 2197–2206.
- 2 a) M. Xue, Y. Yang, X. Chi, Z. Zhang and F. Huang, *Acc. Chem. Res.*, 2012, **45**, 1294–1308; b) T. Ogoshi and T. Yamagishi, *Chem. Commun.*, 2014, **50**, 4776–4787; c) C. Li, *Chem. Commun.*, 2014, **50**, 12420–12433; d) T. Ogoshi, T. A. Yamagishi and Y. Nakamoto, *Chem. Rev.*, 2016, **116**, 7937–8002; e) K. Yang, Y. Pei, J. Wen, and Z. Pei, *Chem. Commun.*, 2016, **52**, 9316–9326; f) T. Kakuta, T. A. Yamagishi and T. Ogoshi, *Acc. Chem. Res.*, 2018, **51**, 1656–1666.
- 3 B. Cheng and A. E. Kaifer, *J. Am. Chem. Soc.*, 2015, **137**, 9788–9791.
- 4 a) Z. Zhu, M. Hong, D. Guo, J. Shi, Z. Tao and J. Chen, *J. Am. Chem. Soc.*, 2014, **136**, 16461–16464; b) W. Xiong, W. Huang, M. Zhang, P. Hu, H. Cui and Q. Zhang, *Chem. Mater.*, 2019, **31**, 8069–8075; c) H. Sun, W. Xiong, W. Zhou, W. Zhang, L. Wang and W. Huang, *Org. Electron.*, 2020, **83**, 105743–105747.
- 5 M. R. Aveil, S. Etezadi, B. Captain and A. E. Kaifer, *Commun. Chem.*, 2020, **3**, 117–131.
- 6 C. Tsuneishi, Y. Koizumi, R. Sueto, H. Nishiyama, K. Yasuhara, T. Yamagishi, T. Ogoshi, I. Tomita and S. Inagi, *Chem. Commun.*, 2017, **53**, 7454–7456.
- 7 K. I. Shivakumar and G. J. Sanjayan, *Synthesis*, 2013, **45**, 896–898.
- 8 T. Ogoshi, K. Yoshikoshi, R. Sueto, H. Nishihara and T. Yamagishi, *Angew. Chem. Int. Ed.*, 2015, **54**, 6466–6469.
- 9 Y. Ma, X. Chi, X. Yan, J. Liu, Y. Yao, W. Chen, F. Huang and J. L. Hou, *Org. Lett.*, 2012, **14**, 1532–1535.
- 10 K. –U. Lao and C. –H. Yu, *J. Comput. Chem.*, 2011, **32**, 2716–2726.
- 11 I. Colomer, C. Batchelor-McAuley, B. Odell, T. J. Donohoe, T. J. Compton and R. G. Compton, *J. Am. Chem. Soc.*, 2016, **138**, 8855–8861.